Electronic and magnetic properties of FeSe thin film prepared on GaAs (001) substrate by metal-organic chemical vapor deposition

K. W. Liu[a)]
Key Laboratory of Excited State Processes, Changchun Insititute of Optics, Fine Mechanics and Physics, Chinese Academy of Sciences, Changchun 130033, China and Graduate School of the Chinese Academy of Sciences, Beijing 100049, China

J. Y. Zhang, D. Z. Shen, C. X. Shan, B. H. Li, Y. M. Lu, and X. W. Fan
Key Laboratory of Excited State Processes, Changchun Insititute of Optics, Fine Mechanics and Physics, Chinese Academy of Sciences, Changchun 130033, China

(Received 24 April 2007; accepted 29 May 2007; published online 25 June 2007)

FeSe film was prepared on GaAs (001) substrate by low pressure metal-organic chemical vapor deposition. The x-ray diffraction measurement indicated that the sample was preferentially oriented with tetragonal structure. The structure relationship between FeSe epilayer and GaAs (001) substrate has been studied. The critical behavior in the temperature-dependent resistivity at ~290 K is close to the Curie temperature, which confirmed that the transformation from ferromagnetism to paramagnetism could be responsible for the critical behavior. © *2007 American Institute of Physics*. [DOI: 10.1063/1.2751578]

Hybrid ferromagnet/semiconductor structures are of strong interest to the development of spintronic devices.[1] For preparing these devices, high quality ferromagnetic thin films are necessary. Up to now, much attention has been concentrated on fabricating high quality ferromagnetic epitaxial films on semiconductor substrates which is one of key factors to make spintronic devices. Many magnetic materials including diluted magnetic semiconductors [e.g., ZnFeSe (Refs. 2 and 3)] and metallic/semimetallic ferromagnets [e.g., Fe,[4] MnAs,[5,6] MnSb (Ref. 7)] have been grown on GaAs substrates. FeSe, as a magnetic material with Curie temperature above room temperature, also could be grown on GaAs substrates. Several methods have been attempted to prepare the iron selenide thin films: molecular beam epitaxy,[8,9] milling pure elemental powders of iron and selenium,[10–12] and selenization of evaporated iron thin films.[13] Most of the Fe–Se compounds were prepared by a two-step method: first fabricating Fe and second selenization.[8,13] The samples fabricated by selenization technique usually have many different phases and bad quality of crystal. Therefore, it is difficult to study the properties of the single phase FeSe. In our previous work,[14–16] high oriented single phase FeSe thin films were fabricated by metal-organic chemical vapor deposition and the electronic and magnetic properties have been studied. The Hall measurement indicated that the as-grown FeSe thin film[15] was of *p*-type conduction with hole concentration of as high as 10^{20}–10^{21} cm^{-3}. We found that the properties of FeSe films are sensitive to the growth conditions, and the critical behavior in the temperature-dependent resistivity characteristics has been observed around 290 K for $Fe_{0.48}Se_{0.52}$.[16] However, the relationship between electronic and magnetic properties of FeSe films is still not clear. Meanwhile, little of information about the magnetic anisotropy which is one of the important parameter for the application of spintronic devices can be observed.

In this letter, we present the structural, electrical, and magnetic properties of FeSe film fabricated by low pressure metal-organic chemical vapor deposition (LP-MOCVD). It is found that FeSe thin films are ferromagnetic with the Curie temperature (T_C) around 305 K. The temperature-dependent resistivity is measured using a four-probe method with annealed indium pads as Ohmic contacts. The epitaxial relationship, $(00l)_{FeSe}\|(00l)_{GaAs}$, between FeSe epilayer and GaAs substrate was also studied. Superconducting quantum interference device (SQUID) and vibrating sample magnetometry (VSM) measurements were performed to characterize the magnetic properties of the FeSe thin film.

FeSe thin film was prepared on GaAs substrate by a LP-MOCVD system with a horizontal rectangular quartz reactor. The ironpentacarbonyl [$Fe(CO)_5$] carried by hydrogen was used as Fe source. The source was kept at 10 °C during deposition. The hydrogen selenide (H_2Se) diluted by high purity hydrogen (10% H_2Se) was selected as source material of Se. The GaAs substrates were semi-insulating with (001) orientation. Before loading, they were cleaned by trichloroethylene, acetone, and ethanol for 5 min in an ultrasonic bath and etched in an sulfuric peroxide solution ($3H_2SO_4+1H_2O_2+1H_2O$) for 5 min at 20 °C. Subsequently, the substrate was boiled in hydrochloric acid for 5 min, followed by a de-ionized water rinsing. Then the growth was performed at 260 °C with the pressure of 150 Torr. The gas flow rates of $Fe(CO)_5$ and H_2Se were fixed at 3 and 18 ml/min. The thickness of the film is about 350 nm and the growth rate is 11 nm/min.

A Rigaku O/max-RA x-ray diffractometer (XRD) with Cu $K\alpha$ radiation ($\lambda=0.154178$ nm) was used to make $\theta-2\theta$ scans to evaluate the crystalline quality and study the structure properties of the FeSe film. Figure 1(a) shows the XRD spectra of the FeSe prepared on GaAs substrate by LP-MOCVD. Besides the diffraction peaks of GaAs substrate at 31.68° and 68.06°, three peaks at 32.61°, 49.78°, and 68.23° of the sample were observed. According to early reports, Fe–Se system has two homogeneous and stable phases at the room temperature, α-FeSe (isotropic with PbO

[a)]Electronic mail: liukewei23@sohu.com

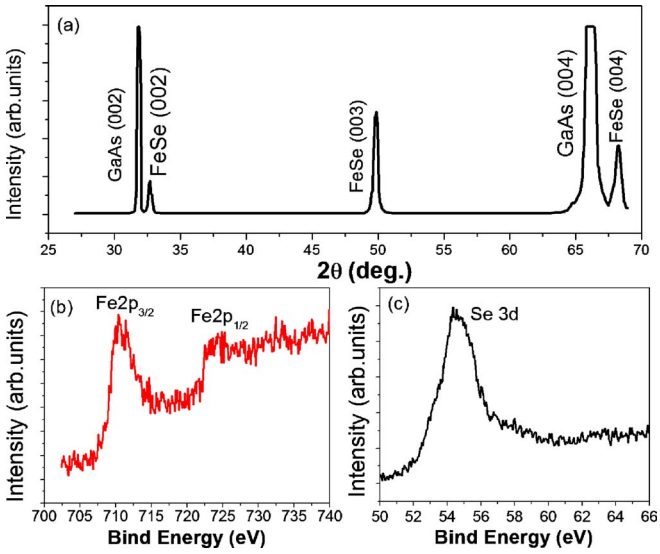

FIG. 1. (Color online) (a) XRD spectra of the FeSe thin film grown on GaAs (001) substrate. XPS spectrum of (b) Fe 2*p* and (c) Se 3*d*.

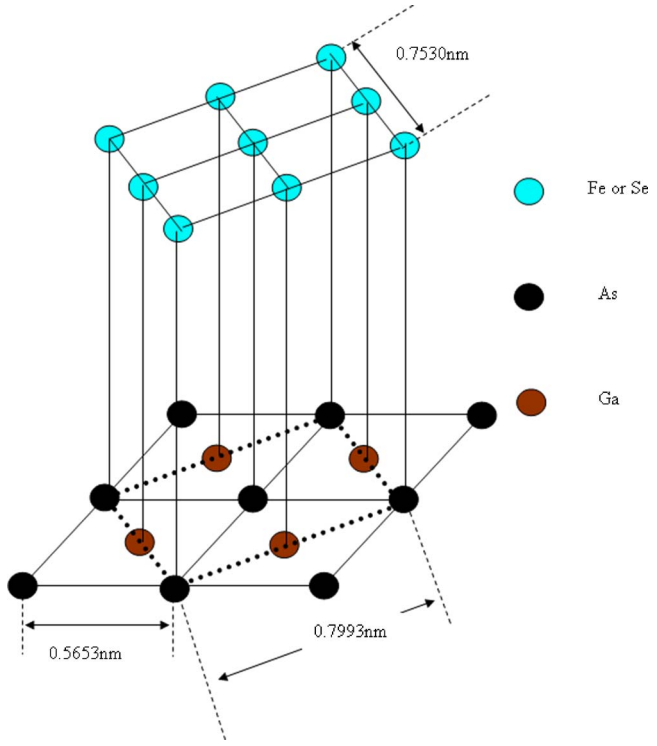

FIG. 2. (Color online) Schematic diagram of a tetragonal structure α-FeSe epilayer with a *c*-face tensile strained state grown on a GaAs (001) substrate.

structure, *B*10) with lattice parameters $a=0.3765$ nm and $c=0.5518$ nm and $FeSe_2$ (isotropic with FeS_2 marcasite structure) with lattice parameters $a=0.3575$ nm, $b=0.4791$ nm, and $c=0.5715$ nm. Energy dispersive spectrometer (EDS) result indicated that the atomic molar ratio of Fe/Se is $(46.9\pm0.5)/(53.1\pm0.5)$. Therefore, three peaks at 32.61°, 49.78°, and 68.23° can be associated with the diffraction from (002), (003), and (004) planes of the α-FeSe with tetragonal structure, and there are some Fe vacancies in FeSe film based on the EDS result. This appearance of only (00l) diffraction peaks indicates that the sample was preferentially oriented. Figures 1(b) and 1(c) showed x-ray photoemission spectroscopy (XPS) spectra of the FeSe thin film grown on GaAs substrate. The surface of the sample was cleaned with 3 keV Ar^+ for 5 min before detection. In Fig. 1(b), the binding energy peaks situated at 710.75 and 723.96 eV can be attributed to Fe $2p_{3/2}$ and Fe $2p_{1/2}$ of iron selenide, and there is no pure Fe phase could be detected in FeSe film. The photoemission spectra of Se 3*d* were presented in Fig. 1(c). The peak at 54.6 eV corresponds to Se 3d of iron selenide and no other phase such as pure Se or selenium oxide occurred in spectra. This result and the results of XRD and EDS indicated that the FeSe film has single phase and was preferentially oriented.

The *c*-axis lattice constant of the FeSe film can be obtained from the diffraction angle by the formula $2d \sin\theta = n\lambda$. From the experimentally measured positions of (002), (003), and (004) diffraction peaks, we have calculated that the *c*-axis lattice constant is about 0.5498 nm, which is a little smaller than 0.5518 nm (bulk FeSe).[17] Little of Fe vacancies can be responsible for this slight decrease of perpendicular component of lattice constant. A possible schematic diagram of the crystal structure for the FeSe/GaAs heterostructure, taking into account for the strain effect is shown in Fig. 2. The epitaxial relationship indicated that the (00l) orientation of FeSe is perpendicular to the surface of GaAs. According to this figure, $2a_{FeSe}$ $(2\times0.3765=0.7530$ nm) is smaller than $\sqrt{2}a_{GaAs}$ $(\sqrt{2}\times0.5653=0.7993$ nm) and the in-plane lattice mismatch between FeSe and GaAs is 5.79%. Therefore, the strain effect occurred in *c* face of FeSe film may be another possible reason which could be responsible for the little decrease of the *c* axis lattice constant of FeSe film.

Temperature-dependent resistivity curve of FeSe thin film was shown in Fig. 3(a). In this figure, the resistivity curves as a function of temperature show a typical metallic behavior at cool state, while a semiconducting behavior at high temperature. The high temperature region was fit independently to an activated form, $\rho(T)=\rho_0\exp(\Delta/k_BT)$, where ρ_0 is the value of resistivity when *T* is large, just as shown in Fig. 3(b). The result of this fit is in excellent agreement with semiconducting model. Meanwhile, in Fig. 3(a), the resistivity curve shows the peak at ~290 K. This result well accorded with Ref. 18. This critical behavior in the

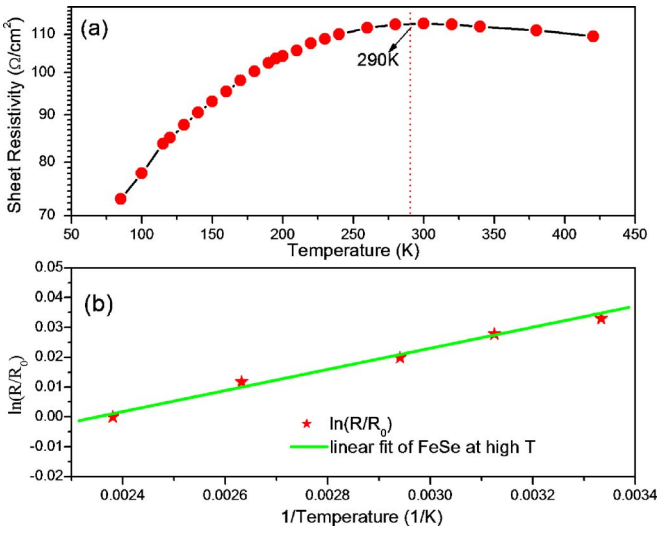

FIG. 3. (Color online) (a) Temperature-dependent resistivity curve of FeSe thin film prepared on GaAs (001) substrate. (b) Fit of resistivity vs temperature to activated form in FeSe at the temperature above 290 K.

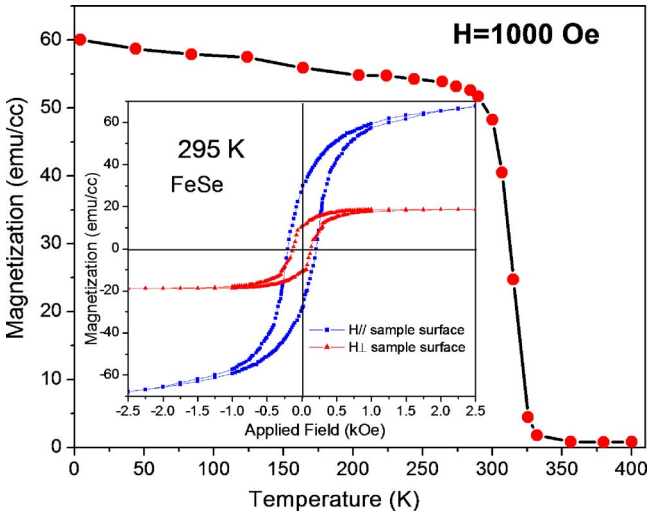

FIG. 4. (Color online) Magnetization curve as a function of the temperature for the FeSe film with the 1000 Oe applied field parallel to the sample surface. The inset shows the magnetization vs applied field curves at 295 K for FeSe film. The curves with filled circles and triangles represent the field directions parallel and perpendicular to the sample surfaces, respectively.

temperature-dependent resistivity characteristics is commonly observed at the temperature region around the T_C of ferromagnetic semiconductors, and this phenomenon is ascribed to the scattering of carriers by the magnetic spin fluctuation via exchange interactions. Therefore, it is expected that the magnetic properties near the room temperature is strongly fluctuated by the thermal energy. Figure 4 shows the magnetization curve as a function of temperature with 1000 Oe applied field parallel to the sample surface. In this figure, the FeSe thin film exhibits the ferromagnetic behavior in the temperature range of 5–330 K as measured by SQUID magnetometer and the abrupt increase of magnetization was observed from 330 to 280 K. Thus the T_C of FeSe film is expected to be about 305 K. The critical behavior in the temperature-dependent resistivity at ~290 K is closed to the T_C value. This result confirmed that the transformation from ferromagnetism to paramagnetism could be responsible for the critical behavior.

The in-plane and out-of-plane field-dependent magnetization measurements of the FeSe film were carried out at 295 K by a VSM (see inset of Fig. 4). Typical hysteresis loops indicated that there is only one ferromagnetic phase in our sample. From this figure, it can be found that the out-of-plane hysteresis loop has lower coercivity (H_C) and more clearly squared shape than that of in-plane. Meanwhile, the out-of-plane hysteresis loops approach the saturation point faster than the in-plane. Furthermore, it should be noted that the 210 Oe coercivity and 62 emu/cc saturation magnetization for in-plane hysteresis loop are smaller than that of Ref. 8, 9, and 15. The growth temperature, the molar ratio of Fe/Se, and the Fe vacancies may be attributed to this differences. Meanwhile, it is noteworthy that the T_C and H_C obtained for FeSe film are not due to the presence of other phases such as Fe_3Se_4 ($T_C \sim 314$ K and $H_C \sim 300$ Oe) and Fe_7Se_8 ($T_C \sim 455$ K and $H_C \sim 2200$ Oe), which is in good agreement with the XRD result.

In conclusion, FeSe thin film was prepared on GaAs(001) substrate by LP-MOCVD. The composition ratio of Fe/Se in FeSe film was measured to be $(46.9 \pm 0.5)/(53.1 \pm 0.5)$. Meanwhile, the critical behavior in the temperature-dependent resistivity characteristics is observed around 290 K and fit of resistivity versus temperature to activated form in FeSe at high temperature (above 290 K) is in good agreement with semiconducting model. The transformation from ferromagnetism to paramagnetism could be responsible for the critical behavior.

This work was supported by the Key Project of National Natural Science Foundation of China under Grant Nos. 60336020 and 50532050 and the Innovation Project of Chinese Academy of Sciences. The National Natural Science Foundation of China under Grant Nos. 50402016 and 60506014.

[1] G. A. Prinz, Science **250**, 1092 (1990).
[2] B. T. Jonker, J. J. Krebs, S. B. Qadri, and G. A. Prinz, Appl. Phys. Lett. **50**, 848 (1987).
[3] B. T. Jonker, J. J. Krebs, S. B. Qadri, G. A. Prinz, F. Volkening, and N. C. Koon, J. Appl. Phys. **63**, 3303 (1988).
[4] Y. Chye, V. Huard, M. E. White, and P. M. Petroff, Appl. Phys. Lett. **80**, 449 (2002).
[5] F. Schippan, G. Behme, L. Däweritz, K. H. Ploog, B. Dennis, K.-U. Neumann, and K. R. A. Ziebeck, J. Appl. Phys. **88**, 2766 (2000).
[6] Tae Whan Kim, Hee Chang Jeon, Tae Won Kang, Ho Seong Lee, Jeong Yong Lee, and Sungho Jin, Appl. Phys. Lett. **88**, 021915 (2006).
[7] B. L. Low, C. K. Ong, J. Lin, A. C. H. Huan, H. Gong, and T. Y. F. Liew, J. Appl. Phys. **85**, 7340 (1999).
[8] Y. Takemura, H. Suto, N. Honda, and K. Kakuno, J. Appl. Phys. **81**, 5177 (1997).
[9] Y. Takemura, N. Honda, T. Takahashi, H. Suto, and K. Kakuno, J. Magn. Magn. Mater. **177-181**, 1319 (1998).
[10] C. E. M. Campos, J. C. de Lima, T. A. Grandi, K. D. Machado, V. Drago, and P. S. Pizani, J. Magn. Magn. Mater. **270**, 89 (2004).
[11] C. E. M. Campos, J. C. de Lima, T. A. Grandi, K. D. Machado, and P. S. Pizani, Solid State Commun. **123**, 179 (2002).
[12] C. E. M. Campos, V. Drago, J. C. de Lima, T. A. Grandi, K. D. Machado, and M. R. Silva, J. Magn. Magn. Mater. **269**, 6 (2004).
[13] N. Hamdadou, J. C. Bernede, and A. Khelil, J. Cryst. Growth **241**, 313 (2002).
[14] Q. J. Feng, D. Z. Shen, J. Y. Zhang, C. X. Shan, Y. M. Lu, Y. C. Liu, and X. W. Fan, J. Magn. Magn. Mater. **279**, 435 (2004).
[15] Q. J. Feng, D. Z. Shen, J. Y. Zhang, C. X. Shan, Y. M. Lu, Y. C. Liu, and X. W. Fan, Appl. Phys. Lett. **88**, 012505 (2006).
[16] K. W. Liu, J. Y. Zhang, Binghui Li, Bingsheng Li, C. X. Shan, Youming Lu, and Dezhen Shen, J. Vac. Sci. Technol. A **25**, 232 (2007).
[17] JCPDS Card No. 85-0735 (unpublished).
[18] N. R. Akhmedov, N. Z. Dzhalilov, and D. Sh. Abdinov, Inorg. Mater. **9**, 1271 (1973).